

Wetting of Cu Pads by Bi-2.6Ag-xCu Alloys and Phase Equilibria in the Ag-Bi-Cu System

PRZEMYSŁAW FIMA,^{1,2} GRZEGORZ GARZEL,¹ and ANNA SYPIEŃ¹

1.—Institute of Metallurgy and Materials Science, Polish Academy of Sciences, ul. Reymonta 25, 30-059 Kraków, Poland. 2.—e-mail: p.fima@imim.pl

The phase equilibrium in the Ag-Bi-Cu system was experimentally determined at 573 K, 773 K, and 973 K by scanning electron microscopy (SEM) and energy dispersive spectroscopy (EDS) on annealed alloys and liquid/solid couples. The experimental results indicate that the mutual solubility of the components is limited. Based on the present results and literature data, phase equilibria in the Ag-Bi-Cu system were thermodynamically assessed. Wetting of Bi-2.6Ag-xCu alloys on Cu substrates was studied with the sessile drop method in the presence of flux at 573 K and 623 K. It was found that the wetting to non-wetting transition corresponds to the solubility limit of Cu in liquid. Selected solidified solder-substrate couples were cross-sectioned and their interfacial microstructure examined with SEM-EDS. There are no reaction products at the interface, but the copper surface becomes rough because of dissolution by liquid solder.

Key words: Ag-Bi-Cu system, microstructure, phase equilibria, wetting

INTRODUCTION

The Bi-Ag eutectic-based alloys are considered a possible replacement for high temperature solders based on Pb.¹ The Bi-Ag eutectic has an acceptable melting point, reasonable cost, and similar hardness to that of Pb-5Sn,² however, it is prone to brittleness³ and its thermal and electrical conductivity should be improved. It was shown that the increase of Ag content to 11 wt.% results in higher thermal⁴ and electrical conductivity.² Unfortunately, it is accompanied with the increase of liquidus temperature and about a 100-K gap between the solidus and liquidus,^{4,5} which has to be considered during actual soldering process. Modification of Bi-Ag eutectic alloy with a third component is also supposed to improve its mechanical, electrical, thermal, and wetting properties. It was⁶ revealed that the addition of Sn to Bi-Ag eutectic improves its wetting on copper. The data on wetting of Cu by Bi-rich Bi-Ag alloys are limited⁶⁻⁹ and differ with respect to reported values of the wetting angle. One important factor affecting quality of the joint, in particular its

mechanical properties, is the structure of connection at the interface.¹⁰ Previous reports show that the interface between the Cu and Bi-Ag alloys is different from the interfaces between Cu and alloys based on Sn or Zn. In particular, no interlayers can be distinguished and dissolution of Cu substrate in Bi-Ag alloy is observed.^{6,11} From a practical point of view, it would be valuable to investigate the effect of the initial Cu content in the alloy on its wetting of Cu substrate and the microstructure of the solder-substrate interface.

The Ag-Bi-Cu system is a part of Ag-Bi-Cu-Sn system also considered as soldering material.¹² Over the past years, attention has been paid to thermodynamics and phase equilibria in the following ternary systems: Ag-Bi-Sn,¹³ Ag-Cu-Sn,^{14,15} and Bi-Cu-Sn.¹⁶ Recent experimental information on the thermal behavior of Ag-Bi-Cu alloys¹⁷ and the thermodynamics of liquid¹⁸ facilitates an assessment of the thermodynamic properties of this system. Therefore, the aim of this work is: (1) to experimentally study phase equilibria in the Ag-Bi-Cu system, (2) to assess the phase diagram of the ternary Ag-Bi-Cu system, and (3) to investigate the effect of Cu concentration on the wettability of Bi-Ag eutectic-based solder alloys on the Cu substrate

(Received March 17, 2014; accepted June 26, 2014; published online July 29, 2014)

with the presence of the flux, and to characterize the microstructure of the interface between solders and the Cu substrate.

EXPERIMENTAL PROCEDURE

Pure metals Ag (99.99 wt.%), Bi (99.999 wt.%), and Cu (99.999 wt.%) were used for the preparation of the alloys. In order to ensure good mixing of the samples and to limit bismuth evaporation, the alloys were prepared by induction melting¹⁹ in graphite crucibles. The as-cast alloys were then cut into smaller pieces and sealed in quartz capsules filled with Ar (99.999%) gas. In order to obtain equilibrated alloys, the samples were annealed at 573 K, 773 K, and 973 K for 2 weeks, while the liquid/solid couples were annealed for 1 h, and 2 h, respectively. After the designated annealing time, the ampoules were quenched in cold water. Compositions of the studied samples are listed in Table I and their positions imposed on a liquidus projection calculated from binary data¹⁵ in Fig. 1. After this heat treatment, the samples were cut, ground, polished, and subjected to microstructure and composition analysis with EDS technique. The EDS analysis was performed at 25 kV, working distance (WD) 10 μm , with the use of the FEI XL30 and standardless analysis EDAX system based on Genesis 2000 software.

For the wettability study, alloys based on Bi-2.6Ag (wt.%) hypereutectic alloy containing 0.63 wt.%, 0.95 wt.%, 1.61 wt.%, and 1.95 wt.% addition of Cu were prepared by melting pure components in graphite crucibles in a resistance furnace under an Ar (99.9992%) protective atmosphere. The as-cast alloys were cut into suitable pieces of approximately 0.3 g and degreased with acetone prior to the wetting tests. Except for degreasing, there was no special treatment of substrates (25 \times 20 \times 0.2 mm). The wetting tests were carried out at 573 K and 623 K on copper substrates, respectively, with the setup used earlier in studies of Bi-Ag-Sn and Bi-Ag-Zn alloys.⁶ The time of contact between the molten sample and the Cu substrate was 60 s. The advantage of this setup is that it enables quick transfer of the sample to the already heated furnace, so the heating rate is very fast, as well as quick transfer out after the designated time of the test.

Wetting tests were performed with ALU33[®] flux applied to the solder sample and the surrounding part of the substrate. According to ISO 9454-1, this is the 2.1.2-type flux, i.e. organic, water-soluble, and activated with halides. Its components are aminothylethanolamine (C₄H₁₂N₂O) and ammonium fluoroborate (NH₄BF₄). The reported wetting angles are the average of three independent measurements on solidified samples after washing the flux residue with tap water. It was not possible to measure molten samples because the flux layer is not transparent to light and obscures the triple line. After the

Table I. Phases in equilibrium in the Ag-Bi-Cu system (present work)

Sample	Temp (K)	Alloys and couples (at.%)	Annealing time	Phase equilibria											
				Phase1			Phase2			Phase3					
				Ag	Bi	Cu	Ag	Bi	Cu	Ag	Bi	Cu			
A3	573	Ag30Bi30Cu40 (alloy)	14 days	Phase1/Phase2/Phase3			Phase2			Phase3					
B3		fcc_(Cu)/fcc_(Ag)/liquid		Ag	Bi	Cu	Ag	Bi	Cu	Ag	Bi	Cu			
H3		fcc_(Cu)/liquid		97.6	2.4	100.0	97.6	2.4	100.0	5.7	94.3	—			
A5	773	Ag4Bi76Cu20 (alloy)	14 days	Phase1/Phase2/Phase3			Phase2			Phase3					
B5		fcc_(Cu)/fcc_(Ag)/liquid		Ag	Bi	Cu	Ag	Bi	Cu	Ag	Bi	Cu			
H5		fcc_(Cu)/liquid		3.8	93.2	3.0	3.8	93.2	3.0	6.5	93.5	—			
A7	973	Ag15Bi15Cu70 (alloy)	14 days	Phase1/Phase2/Phase3			Phase2			Phase3					
B7		fcc_(Cu)/fcc_(Ag)/liquid		Ag	Bi	Cu	Ag	Bi	Cu	Ag	Bi	Cu			
H7		fcc_(Cu)/liquid		94.7	2.4	2.9	94.7	2.4	2.9	6.5	93.5	—			
A5	773	Ag30Bi30Cu40 (alloy)	14 days	Phase1/Phase2/Phase3			Phase2			Phase3					
B5		fcc_(Cu)/fcc_(Ag)/liquid		Ag	Bi	Cu	Ag	Bi	Cu	Ag	Bi	Cu			
H5		fcc_(Cu)/liquid		50.4	39.9	9.7	50.4	39.9	9.7	6.9	93.5	—			
A5	773	Ag4Bi76Cu20 (alloy)	14 days	Phase1/Phase2/Phase3			Phase2			Phase3					
B5		fcc_(Cu)/fcc_(Ag)/liquid		Ag	Bi	Cu	Ag	Bi	Cu	Ag	Bi	Cu			
H5		fcc_(Cu)/liquid		5.7	87.4	6.9	5.7	87.4	6.9	6.9	93.5	—			
C5	973	Ag48Bi12Cu40 (alloy)	14 days	Phase1/Phase2/Phase3			Phase2			Phase3					
D5		fcc_(Cu)/fcc_(Ag)/liquid		Ag	Bi	Cu	Ag	Bi	Cu	Ag	Bi	Cu			
E5		fcc_(Cu)/liquid		0.6	99.4	99.4	0.6	99.4	99.4	61.7	26.9	11.4			
D5	973	Ag50Bi50/Cu (couple)	2 h	Phase1/Phase2/Phase3			Phase2			Phase3					
E5		Cu/liquid		Ag	Bi	Cu	Ag	Bi	Cu	Ag	Bi	Cu			
A7		Cu/fcc_(Ag)/liquid		100.0	100.0	13.8	100.0	100.0	13.8	72.6	18.0	9.4			
A7	973	Ag75Bi25/Cu (couple)	2 h	Phase1/Phase2/Phase3			Phase2			Phase3					
C7		fcc_(Cu)/liquid		Ag	Bi	Cu	Ag	Bi	Cu	Ag	Bi	Cu			
D7		fcc_(Cu)/liquid		1.5	98.5	98.5	1.5	98.5	98.5	4.4	94.3	—			
C7	973	Ag30Bi30Cu40 (alloy)	14 days	Phase1/Phase2/Phase3			Phase2			Phase3					
D7		fcc_(Cu)/fcc_(Ag)/liquid		Ag	Bi	Cu	Ag	Bi	Cu	Ag	Bi	Cu			
E7		fcc_(Cu)/liquid		58.9	14.9	26.2	58.9	14.9	26.2	14.7	85.3	—			
C7	973	Ag48Bi12Cu40 (alloy)	14 days	Phase1/Phase2/Phase3			Phase2			Phase3					
D7		fcc_(Cu)/fcc_(Ag)/liquid		Ag	Bi	Cu	Ag	Bi	Cu	Ag	Bi	Cu			
E7		fcc_(Cu)/liquid		92.0	1.7	6.3	92.0	1.7	6.3	14.7	85.3	—			
D7	973	Ag50Bi50/Cu (couple)	1 h	Phase1/Phase2/Phase3			Phase2			Phase3					
E7		Cu/liquid		Ag	Bi	Cu	Ag	Bi	Cu	Ag	Bi	Cu			
A7		Cu/fcc_(Ag)/liquid		100.0	100.0	27.4	100.0	100.0	27.4	27.4	72.6	—			
D7	973	Ag75Bi25/Cu (couple)	1 h	Phase1/Phase2/Phase3			Phase2			Phase3					
E7		Cu/liquid		Ag	Bi	Cu	Ag	Bi	Cu	Ag	Bi	Cu			
A7		Cu/fcc_(Ag)/liquid		54.9	17.8	27.3	54.9	17.8	27.3	27.4	72.6	—			

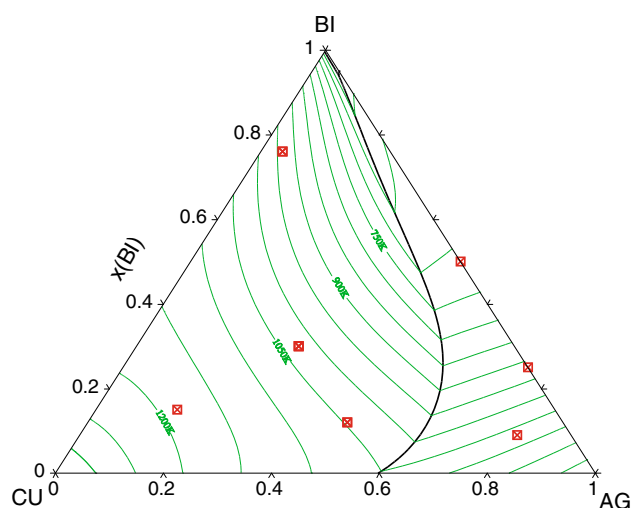


Fig. 1. Liquidus projection calculated from extrapolated binary data.¹⁵ Points denote composition of annealed alloys and liquid/solid couples (Table I).

wetting tests, selected solidified solder/substrate couples were cut perpendicular to the plane of the interface, mounted in conductive resin, and polished for microstructural characterization. The microstructural and energy dispersive spectroscopy (EDS) analysis was performed with the same setup as in the case of the annealed alloys.

PHASE DIAGRAM

Literature Survey

In order to create a thermodynamic description of ternary system, it is necessary to collect thermodynamic descriptions of each of the limiting binary systems. In the case of the Ag-Bi-Cu ternary, each binary constituent system is a simple eutectic one. In the case of the Ag-Bi system, the solubility limit of Bi in the Ag terminal solution is 5 wt.% at 773 K and 2.1 wt.% at 573 K, while in the case of the Ag-Cu system, the mutual solubility of components is much wider at 973 K than at 573 K: respectively, ~5 wt.% and <0.3 wt.%. The Bi-Cu system shows no mutual solubility of components. Thermodynamic descriptions of these systems in the SOLDERS database, developed under the framework of COST Action 531 “Lead-free solder materials”, were, respectively, taken from: Ag-Bi,^{20,21} Ag-Cu,^{21,22} and Bi-Cu.²³ In the case of binaries Ag-Cu²⁴ and Ag-Bi,²⁵ more recent published data reveal the differences between the calculated phase diagrams to be negligible. Also, to keep the present work consistent with the COST-531 database we have decided to adopt the data for binary systems directly, and recalculate integral mixing enthalpy.¹⁸

Experimental information on the phase equilibria in ternary Ag-Bi-Cu alloys were, until recently, limited to just two papers.^{26,27} Zanicchi et al.²⁶ studying supercooling in Ag-Bi-Cu alloys reported the existence of a ternary eutectic at 513 ± 5 K near

the Bi-rich corner without specifying the phases in equilibrium. Liu and Sun,²⁷ based on a DTA study of 12 cross-sections, established a ternary eutectic at 531 K for 5Ag-94.5Bi-0.5Cu (at.%) and proposed the liquidus projection. The liquidus projections were calculated from extrapolated binary data by Kattner²⁸ and Doi et al.¹² Although they used different sets of binary data, the outcomes of their calculations were close and in reasonable agreement with the data of Liu and Sun.²⁷ Recently, we have studied phase transitions with temperature in 24 alloys¹⁷ characterized by fixed molar ratios of Ag to Bi (0.25, 1, 4) and varying copper content, and compared the results with transition temperatures calculated from extrapolated binary data in the SOLDERS database.¹⁵ Good agreement was observed between the experiment and the calculations. Selected as-cast samples were subjected to microstructure characterization, and it was found that the three phases, (Ag), (Bi), and (Cu), show limited solubility of the remaining components. The only thermodynamic data for this ternary system is enthalpy of mixing in liquid phase¹⁸ determined at 1073 K for six cross-sections of fixed molar ratios: Ag/Bi = 0.25, 1, 4; Ag/Cu = 1.5; and Bi/Cu = 1.86, 4. The integral enthalpies of mixing are small and endothermic, similar to limiting binary alloys.

Experimental Phase Equilibria

Figure 1 illustrates the liquidus projection of the Ag-Bi-Cu system with points indicating the composition of alloys subjected to annealing. Figure 2a–d illustrates typical microstructures of selected annealed alloys and the liquid/solid couple. Figure 2a illustrates the microstructure of alloy $\text{Ag}_{30}\text{Bi}_{30}\text{Cu}_{40}$ (at.%) annealed at 573 K for 2 weeks; here, three coexisting phases can be distinguished: liquid, fcc_(Cu), and fcc_(Ag). Figure 2b presents the microstructure of $\text{Ag}_{48}\text{Bi}_{12}\text{Cu}_{40}$ (at.%) alloy annealed at 773 K, where there is a three-phase field: liquid + fcc_(Cu) + fcc_(Ag). Figure 2c illustrates the microstructure of $\text{Ag}_{81}\text{Bi}_9\text{Cu}_{10}$ (at.%) alloy annealed at 973 K, where there is a two-phase field: liquid + fcc_(Ag). In Fig. 2d, the microstructure of the liquid/solid couple $\text{Ag}_{75}\text{Bi}_{25}/\text{Cu}$ after 2 h of annealing at 773 K, the dissolution of solid copper by semi-liquid $\text{Ag}_{75}\text{Bi}_{25}$ (at.%) alloy, is clearly visible.

Thermodynamic Model and Assessment

Since there are no intermetallic phases in the Ag-Bi-Cu ternary system and its binary subsystems, only liquid, fcc_(Ag), fcc_(Cu), and rho_(Bi) exist in the Ag-Bi-Cu system. The Gibbs free energies of these phases are described by the subregular solution model. The molar Gibbs energy of these solutions is expressed as follows:

$$G_m^\phi = \sum_{i=\text{Ag,Bi,Cu}} G_i^\phi x_i + \sum_{i=\text{Ag,Bi,Cu}} x_i \ln x_i + {}^E G_\phi \quad (1)$$

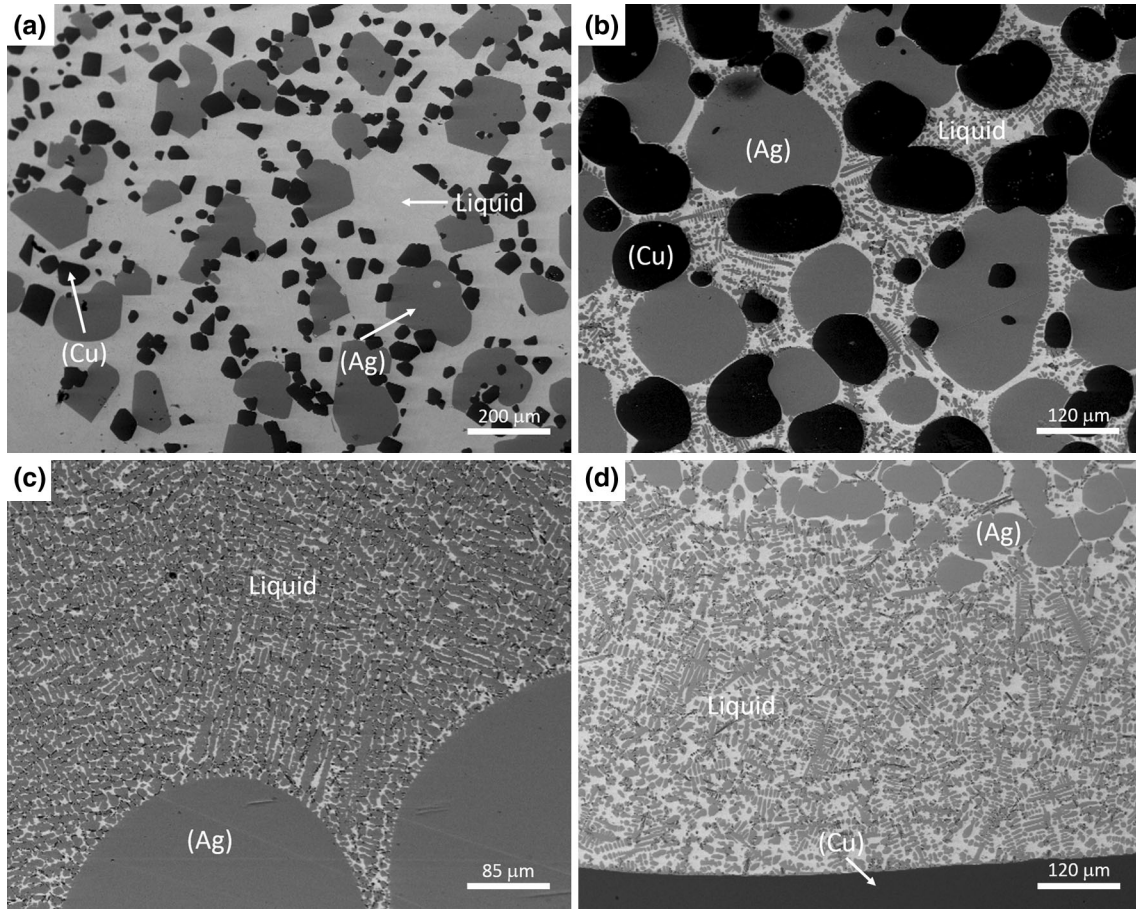


Fig. 2. SEM micrographs of annealed alloys and liquid/solid couples (at.%): (a) $\text{Ag}_{30}\text{Bi}_{30}\text{Cu}_{40}$ at 573 K, (b) $\text{Ag}_{48}\text{Bi}_{12}\text{Cu}_{40}$ at 773 K, (c) $\text{Ag}_{81}\text{Bi}_9\text{Cu}_{10}$ at 973 K, (d) $\text{Ag}_{75}\text{Bi}_{25}/\text{Cu}$ at 773 K.

where x_i denotes the molar fraction of element i ($i = \text{Ag}, \text{Bi}, \text{or Cu}$) in the phase ϕ , and G_i^ϕ is the molar Gibbs energy of the pure component i in ϕ state, which is taken from the SGTE database.

Excess Gibbs energy ${}^E G_\phi$ is formulated with the Redlich–Kister formula^{29,30}:

$$\begin{aligned}
 {}^E G_\phi = & x_{\text{Ag}}x_{\text{Bi}} \sum_{i=0,1,\dots} {}^i L_{\text{Ag,Bi}}^\phi (x_{\text{Ag}} - x_{\text{Bi}})^i + x_{\text{Ag}}x_{\text{Cu}} \\
 & \sum_{i=0,1,\dots} {}^i L_{\text{Ag,Cu}}^\phi (x_{\text{Ag}} - x_{\text{Cu}})^i \\
 & + x_{\text{Bi}}x_{\text{Cu}} \sum_{i=0,1,\dots} {}^i L_{\text{Bi,Cu}}^\phi (x_{\text{Bi}} - x_{\text{Cu}})^i + x_{\text{Ag}}x_{\text{Bi}}x_{\text{Cu}} \\
 & \left(x_{\text{Ag}}^0 L_{\text{Ag,Bi,Cu}}^\phi + x_{\text{Bi}}^1 L_{\text{Ag,Bi,Cu}}^\phi + x_{\text{Cu}}^2 L_{\text{Ag,Bi,Cu}}^\phi \right)
 \end{aligned} \quad (2)$$

where $L_{\text{Ag,Bi}}^\phi$, $L_{\text{Ag,Cu}}^\phi$ and $L_{\text{Bi,Cu}}^\phi$ are the binary interaction parameters cited from.¹⁵

The ternary interaction parameters ${}^0 L_{\text{Ag,Bi,Cu}}^\phi$, ${}^1 L_{\text{Ag,Bi,Cu}}^\phi$ and ${}^2 L_{\text{Ag,Bi,Cu}}^\phi$ are described as follows:

$${}^n L_{\text{Ag,Bi,Cu}}^\phi = a'_n + b'_n T \quad (3)$$

Table II. Thermodynamic parameters of liquid phase in the Ag–Bi–Cu system (present work)

Phase	Parameters (J/mol)
Liquid (Ag, Bi, Cu)	${}^0 L_{\text{Ag,Bi,Cu}}^\phi = -10999.9$ ${}^1 L_{\text{Ag,Bi,Cu}}^\phi = -29105.2$ ${}^2 L_{\text{Ag,Bi,Cu}}^\phi = -35142.9$

where a'_n and b'_n are to be optimized in this work. The best fit to experimental data was obtained when ternary interaction parameters (${}^0 L_{\text{Ag,Bi,Cu}}^\phi$, ${}^1 L_{\text{Ag,Bi,Cu}}^\phi$ and ${}^2 L_{\text{Ag,Bi,Cu}}^\phi$) for solid phases were equal to zero, and the ternary interaction parameters for liquid phase (Table II) were non-zero yet independent on temperature.

Figure 3 presents isopleths calculated for sections of fixed mole fraction ratios of $X(\text{Ag})/X(\text{Bi}) = 0.25, 1, 4$ with the use of new ternary interaction parameters for the liquid phase. Very good agreement between the calculations and the experimental data (points)¹⁷ is visible, in particular in the case of transitions occurring at low temperature.

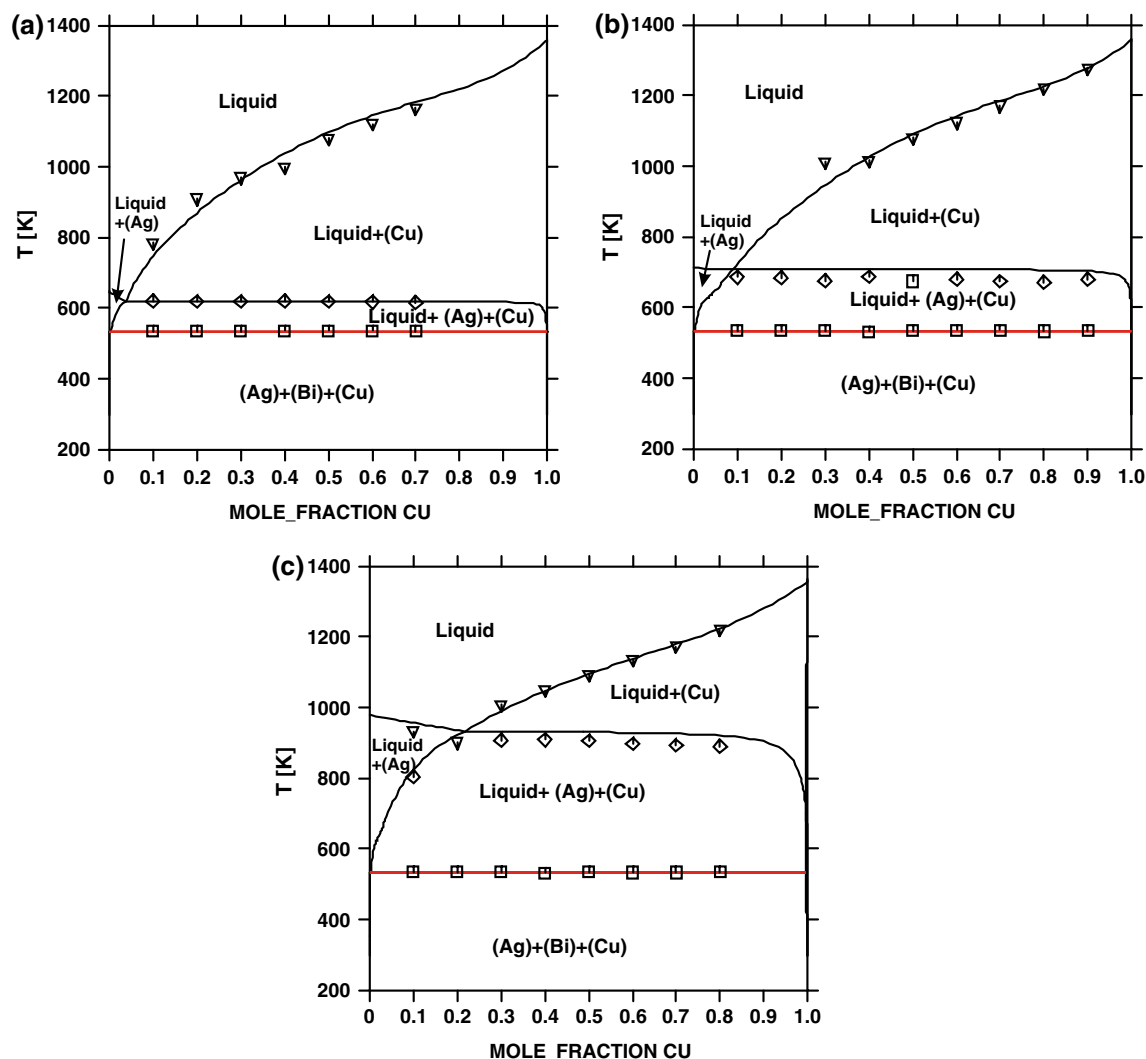


Fig. 3. Isoleths calculated with the assessed thermodynamic parameter for $X(\text{Ag})/X(\text{Bi})$ equal to: (a) 0.25, (b) 1, (c) 4. Points denote experimentally determined DTA data.¹⁷

Isothermal sections of the Ag-Bi-Cu system calculated at 573 K, 773 K, and 973 K (with points imposed indicating the results of the EDS analysis in Table I) are shown in Fig. 4.

Using present set of thermodynamic parameters mixing enthalpy of liquid alloys was calculated at 1073 K for sections: (a) $X(\text{Ag})/X(\text{Bi}) = 1$, (b) $X(\text{Bi})/X(\text{Cu}) = 1.86$. Good agreement was obtained between calculated and experimental data, as can be seen in Fig. 5. Here, lines denote calculated mixing enthalpy and points denote experimental data.¹⁸

WETTING AND INTERFACIAL CHEMISTRY

Figure 6 shows the wetting angle values determined on solidified samples after 60 s of contact between molten Bi-2.6Ag-*x*Cu alloys ($x = 0$ wt.%, 0.63 wt.%, 0.95 wt.%, 1.61 wt.%, 1.95 wt.%) and Cu substrates at 573 K and 623 K, respectively. The results clearly indicate that, at each temperature,

the alloys can be divided into two groups: one with a wetting angle below 90° (wetting the substrate) and the other with a wetting angle above 90° (non-wetting). At 573 K, only the Bi-2.6Ag alloy exhibits a wetting angle below 90° , whereas at 623 K both Bi-2.6Ag and Bi-2.6Ag-0.63Cu exhibit wetting angles below 90° . The wetting angle data in Fig. 6 are the average of measurements on three independent samples per each combination of temperature and composition. One can see that the data are scattered, and this discrepancy can be partly explained by the fact that the wetting angle was measured on solidified samples. In Fig. 7, solidification paths for Bi-2.6Ag, Bi-2.6Ag-0.63Cu, and Bi-2.6Ag-1.95Cu alloys calculated with the lever rule are shown. It can be seen that, at 623 K, the fraction of the solid in Bi-2.6Ag-1.95Cu is above 0.04, in Bi-2.6Ag-0.63Cu it is below 0.005, and in the Bi-2.6Ag fraction of the solid is 0. In general, transition from wetting to non-wetting corresponds to increasing

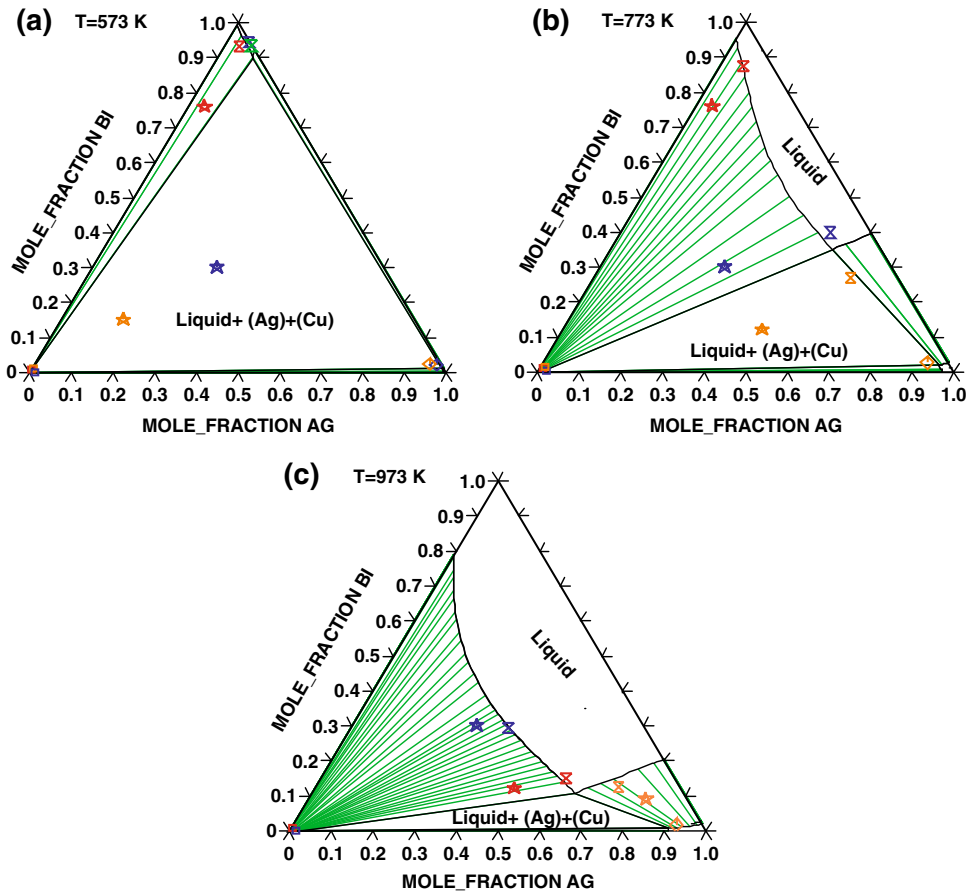


Fig. 4. Isothermal sections calculated from assessed data at: (a) 573 K, (b) 773 K, and (c) 973 K. Points denote respectively: stars the composition of the studied alloys; diamonds, squares, and hourglasses the composition of phases in equilibrium: fcc_(Ag), fcc_(Cu), and liquid, respectively.

concentrations of Cu in the alloy, i.e. alloy compositions showing non-wetting are not fully liquid (fall beyond the liquidus limit). Therefore, it can be speculated that the existence of the solid phase in the alloy (even at a very low level) affects wettability. In the case of Bi-Ag- x Cu alloys, wettability data are limited.^{6,8,9} In Ref. 8, the wetting angle of 40° was reported for Bi-2.5Ag/Cu, after wetting at 613 K for 60 s, but no information on the flux used (if any) was provided. For the same alloy composition⁶ after 60 s at 573 K in the presence of 1.1.2-type flux (rosin low activated with halides), the wetting angle was 64°. The wetting angle after reflow test with similar flux (1.1.2-type) for Bi-2.6Ag-0.1Cu alloy was 58° at 573 K and 50° at 603 K.

Figure 8 illustrates the microstructure of as-cast alloys Bi-2.6Ag, Bi-2.6Ag-0.63Cu, and Bi-2.6Ag-1.95Cu (wt.%), respectively. In the case of the Bi-2.6Ag alloy (Fig. 8a), the microstructure of the sample is eutectic, although a few isolated particles of silver ($\sim 5 \mu\text{m}$) can be found. In the case of Bi-2.6Ag-0.63Cu (Fig. 8b) in the eutectic matrix, there are numerous needle-like precipitates. With EDS analysis, they were found to contain ~ 20 wt.%

Cu, ~ 1 wt.% Ag, and the rest Bi; however, one has to be cautious regarding these results. In the case when two dimensions of the microstructure feature are significantly smaller than the third one, it is very likely that the EDS signal was collected from a volume exceeding the volume of the studied feature. In the case of the Bi-2.6Ag-1.95Cu alloy (Fig. 8c), the number of needle-like features is reduced but precipitates of nearly pure copper are present, randomly distributed in the alloy. The content of Cu dissolved in the Bi-Ag matrix does not exceed 1 wt.%.

The interfacial microstructure after contact for 60 s at 623 K is shown in Fig. 9 for Bi-2.6Ag- x Cu/Cu ($x = 0$ wt.%, 0.63 wt.%, 1.95 wt.%) pairs. In each case, the surface of the substrate is rough and the alloy dissolves the substrate along grain boundaries. This is an example of dissolutive wetting, on which more can be found in Ref. 31. Similar results were obtained for $x = 0.95$ wt.% and 1.63 wt.% Cu at 573 K. Isolated precipitates of Ag can be observed in the vicinity of the substrate, and roughness of the substrate and small precipitates of silver near the interface have also been observed.⁸ Roughening of the substrate is caused by the Bi-Ag ability to

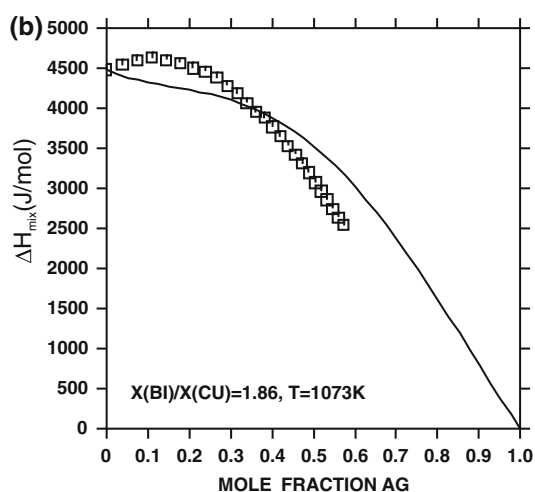
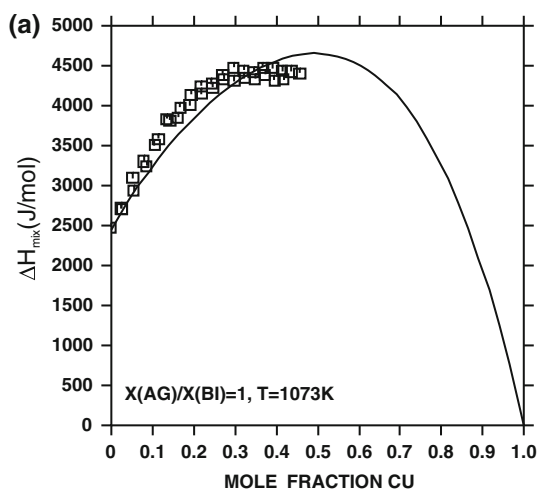


Fig. 5. Enthalpy of mixing for sections: (a) $X(AG)/X(BI) = 1$, (b) $X(BI)/X(CU) = 1.86$. Calculated from assessed data (line) versus experimental data¹⁸ (points).

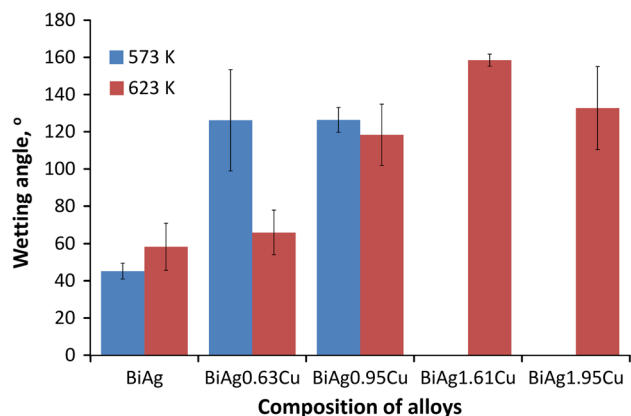


Fig. 6. Contact angle of Bi-Ag-xCu alloys (= 0 wt.%, 0.63 wt.%, 0.95 wt.%, 1.61 wt.%, 1.95 wt.%) at 573 K and 623 K, respectively.

groove the grain boundaries of copper,⁸ and this mechanism is responsible for bonding the substrate and the solder. It should be noted that, in the case of

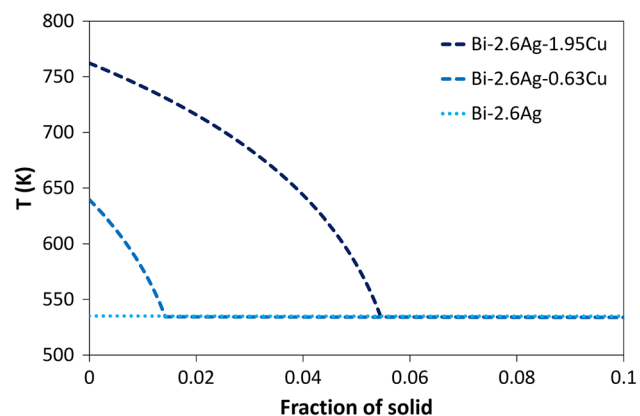


Fig. 7. Solidification path calculated (lever rule) for: Bi-2.6Ag-1.95Cu, Bi-2.6Ag-0.63Cu, and Bi-2.6Ag (wt.%).

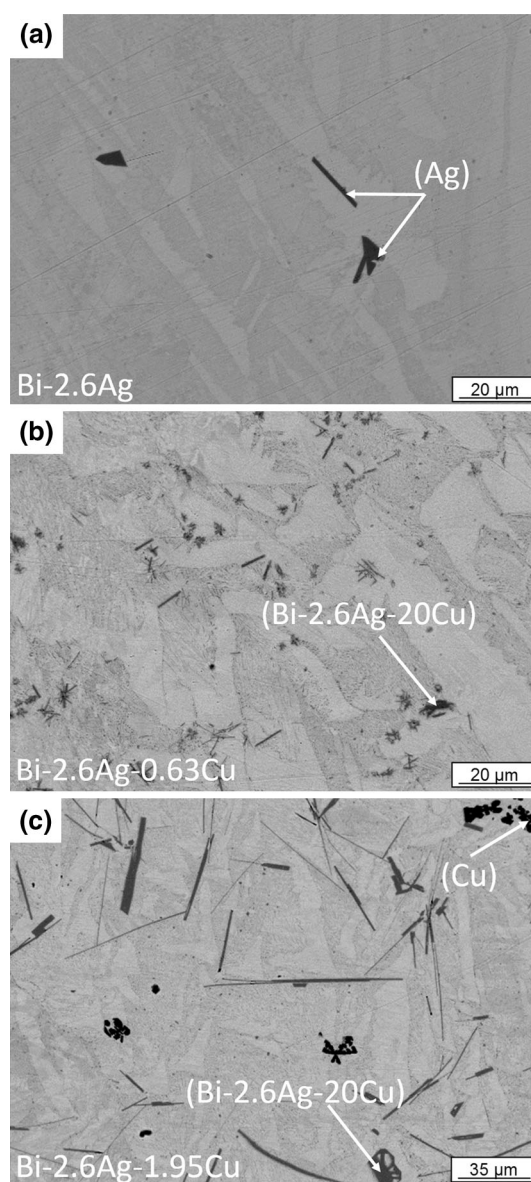


Fig. 8. SEM micrographs of cast alloys: (a) Bi-2.6Ag, (b) Bi-2.6Ag-0.63Cu, and (c) Bi-2.6Ag-1.95Cu.

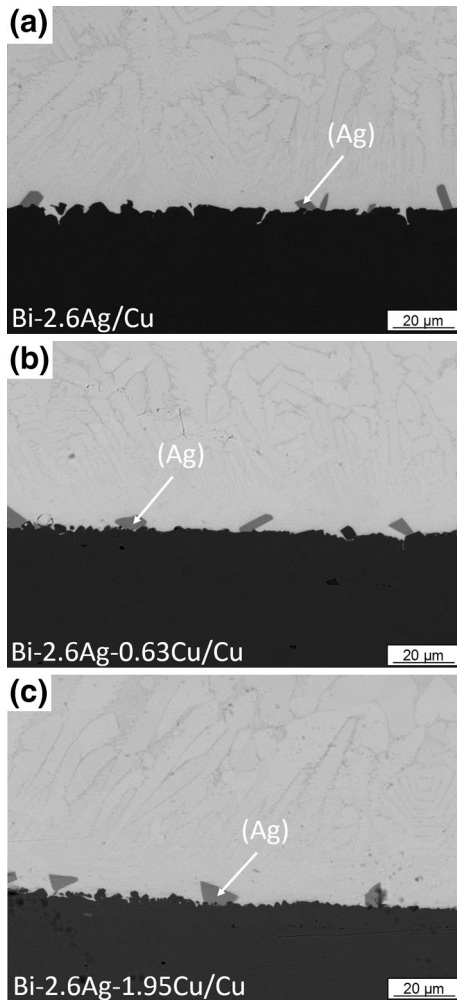


Fig. 9. SEM micrographs of interfacial microstructure: (a) Bi-2.6Ag/Cu, (b) Bi-2.6Ag-0.63Cu/Cu, and (c) Bi-2.6Ag-1.95Cu/Cu.

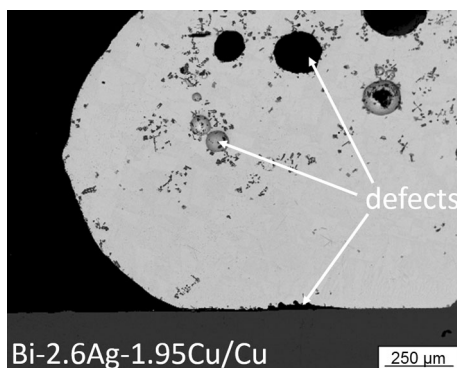


Fig. 10. Low magnification SEM micrograph of Bi-2.6Ag-1.95Cu/Cu.

some of the non-wetting pairs (samples), we observed poor adhesion of solidified drops to the substrate (Fig. 10) (similar to fillet lifting), whereas such defects were not observed for pairs exhibiting wetting.

Joseph et al.³² studied the dissolution and grooving along grain boundaries of copper immersed in pure bismuth and in bismuth nearly saturated with copper (at 873 K, the solubility of copper is ~ 11 wt.%). They observed the dissolution of Cu in both liquids; however grooving along grain boundaries was observed in the case of bismuth saturated with copper. They concluded that, in the case of pure bismuth, the dissolution rate is close to the rate of grooving, whereas once the liquid reaches saturation level the grooving rate is greater than the total rate of dissolution. Song et al.¹¹ studied the dissolution of copper in pure Bi, Bi-2.5Ag, and Bi-11Ag (wt.%). They found that the dissolution of Cu is correlated with the initial concentration of Ag in the solder, i.e., under the same time–temperature conditions, Bi-11Ag dissolves the highest and pure Bi the lowest amounts of copper. From the micrographs, it can be estimated that the difference in substrate roughness is negligible. Thus, it can be speculated that during short time wetting of Bi-2.6Ag- x Cu alloys on a copper substrate, the copper content does not affect the grooving of the substrate.

CONCLUSION

- (1) Isothermal sections of the Ag-Bi-Cu system at 573 K, 773 K, and 973 K were studied by means of SEM and EDS. The experimental results indicate that the mutual solubility of the components is limited.
- (2) A set of thermodynamic parameters for liquid phase, consistent with the SOLDERS database, was derived based on the present experimental and literature data.
- (3) The wetting of Bi-2.6Ag- x Cu alloys on Cu substrates was studied. Ternary alloys do not wet the Cu surface when the initial concentration of Cu in alloy exceeds its solubility limit in liquid. Dissolution of the Cu substrate along grain boundaries is observed regardless of the initial alloy composition.

ACKNOWLEDGEMENT

This work is financed by the Ministry of Science and Higher Education of Poland Grant IP2011 012571 in the years 2012–2014.

OPEN ACCESS

This article is distributed under the terms of the Creative Commons Attribution License which permits any use, distribution, and reproduction in any medium, provided the original author(s) and the source are credited.

REFERENCES

1. K. Suganuma, S.J. Kim, and K.S. Kim, *JOM* 61, 64 (2009).
2. J.M. Song, H.Y. Chuang, and T.X. Wen, *Metall. Mater. Trans. A* 38, 1371 (2007).
3. M. Rettenmayr, P. Lambracht, B. Kempf, and M. Graff, *Adv. Eng. Mater.* 7, 965 (2005).

4. J.H. Lalena, N.F. Dean, and M.W. Weiser, *J. Electron. Mater.* 31, 1244 (2002).
5. R. Kolenak, M. Martinkovic, and M. Kolenakova, *Arch. Metall. Mater.* 58, 529 (2013). doi:10.2478/amm-2013-0031.
6. P. Fima, W. Gasior, A. Sypien, and Z. Moser, *J. Mater. Sci.* 45, 4339 (2010).
7. J.H. Kim, S.W. Jeong, and H.M. Lee, *Mater. Trans.* 43, 1873 (2002).
8. J.M. Song, H.Y. Chuang, and Z.M. Wu, *J. Electron. Mater.* 35, 1041 (2006).
9. B. Kim, C.-W. Lee, D. Lee, and N. Kang, *J. Alloys Compd.* 592, 207 (2014). doi:10.1016/j.jallcom.2013.12.252.
10. N. Sobczak, A. Kudyba, R. Nowak, W. Radziwill, and K. Pietrzak, *Pure Appl. Chem.* 79, 1755 (2007).
11. J.M. Song, H.Y. Chuang, and Z.M. Wu, *J. Electron. Mater.* 36, 1516 (2007).
12. K. Doi, H. Ohtani, and M. Hasebe, *Mater. Trans.* 45, 380 (2004).
13. L.A. Zabdyr and G. Garzel, *Calphad* 33, 187 (2009). doi:10.1016/j.calphad.2008.07.001.
14. A. Dinsdale, A. Watson, A. Kroupa, J. Vrestal, A. Zemanowa, and J. Vizdal, COST Action 531—Atlas of Phase Diagrams for Lead-Free Soldering (Brussels :COST Office, 2008).
15. SOLDERS Database for Lead Free Solders, (<http://www.npl.co.uk/science-technology/advanced-materials/mtdata/databases/materials-specific-databases/>, 2008), Accessed 15 Jan 2014.
16. D. Zivkovic, D. Minic, D. Manasijevic, N. Talijan, I. Katayama, and A. Kostov, *J. Mater. Sci.: Mater. Electron.* 22, 1130 (2011). doi:10.1007/s10854-010-0272-y.
17. P. Fima and G. Garzel, *Calphad* 44, 48 (2014). doi:10.1016/j.calphad.2013.07.011.
18. P. Fima and H. Flandorfer, *Thermochim. Acta* 575, 336 (2014). doi:10.1016/j.tca.2013.11.018.
19. A. Sypien and W. Przybylo, *Mater. Sci. Technol.* 26, 31 (2010). doi:10.1179/174328409X42257.
20. B. Zimmermann (Thesis, University of Stuttgart, 1979).
21. H.L. Lukas and B. Zimmermann (Unpublished work, 1998).
22. F.H. Hayes, H.L. Lukas, G. Effenberg, and G. Petzow, *Z. Metallkd.* 77, 749 (1986).
23. O. Teppo, J. Niemela, and P. Taskinen, *Report TKK-V-B50* (Helsinki University of Technology, 1989).
24. V.T. Witusiewicz, U. Hecht, S.G. Fries, and S. Rex, *J. Alloys Compd.* 385, 133 (2004).
25. U. Kattner and U. Boettinger, *J. Electron. Mater.* 23, 603 (1994).
26. G. Zanichchi, R. Ferro, R. Marazza, and V. Contardi, *J. Less-Common Met.* 50, 151 (1976).
27. S. Liu and W. Sun, *Acta Metall. Sinica (English Ed.)* 2B, 151 (1989).
28. U. Kattner (<http://www.metallurgy.nist.gov/phase/solder/agbicu.html>, 2003). Accessed 15 Jan 2014.
29. O. Redlich and A.T. Kister, *Ind. Eng. Chem.* 40, 354 (1948).
30. Y.-M. Muggianu, M. Gambino, and L.P. Bros, *J. Chim. Phys.* 72, 85 (1975).
31. T.J. Singler, S. Su, L. Yin, and B.T. Murray, *J. Mater. Sci.* 47, 8261 (2012). doi:10.1007/s10853-012-6622-9.
32. B. Joseph, F. Barbier, G. Dagoury, and M. Acouturier, *Scr. Mater.* 39, 775 (1998).